Application of a Magnetic Tracer Method for the Characterization of Hydrodynamics in Internal-Loop Airlift Bioreactors*

J. KLEIN**, O. DOLGOŠ, Š. GODÓ***, M. BLAŽEJ, and J. MARKOŠ

Department of Chemical and Biochemical Engineering, Faculty of Chemical Technology, Slovak University of Technology, SK-812 37 Bratislava
e-mail: jklein@chtf.stuba.sk

Received 19 May 2000

Nowadays there is still a lack of measuring techniques, which would give reliable information about the hydrodynamics in internal-loop airlift reactors (ALR) not only with model media but also during real fermentation processes. Hydrodynamic parameters (liquid residence time distribution, linear circulation velocity, intensity of turbulence) are of particular importance for the verification of the validity of hydrodynamic models or the scale-up procedure. Thus, a magnetic tracer method was developed allowing the measurement of the liquid circulation velocity in individual sections of internal-loop airlift bioreactors during fermentation processes. We attained a signal with a very low noise to signal ratio, which gave reproducible information on the residence time of a magnetic particle in the appropriate section of the ALR. Moreover, the linear liquid circulation velocity, V_L, could be calculated if the settling velocity of the tracer particle was known. The results attained were compared with the pulse response method using hot water. Differences of V_L values between both measuring methods were within ± 20 %. A proper formulation of the effective buoyancy in a gas-liquid dispersion is discussed in this paper. Our results demonstrate that the effective buoyancy is based on the liquid density, so the Archimedes buoyancy force is the proper expression for the formulation of the effective buoyancy. It seems that probably a *critical diameter* of the classifying particle with respect to the diameter of surrounding particles or bubbles exists, which determines the formulation of the effective buoyancy.

In recent years, an increasing number of investigators have attempted to test the use of airlift reactors (ALR) in biotechnology. Despite their simple construction, the usage of ALR is still limited due to several reasons. The most important reason is the lack of hydrodynamic models, which can be applied also to the description of the behaviour of fermentation broths. Models based on energy [1] and momentum [2] balances seem to be general, however, the involved empirical loss and hold-up terms are not well established. The next reason of the limited use of ALR is the lack of measuring techniques, which would give reliable information on the hydrodynamic behaviour in ALRs with model media as well as during real fermentation processes. Hydrodynamic parameters (*e.g.* liquid residence time distribution, linear circulation velocity, intensity of turbulence) are of particular importance for the verification of the validity of hydrodynamic models or the scale-up procedure.

Bioreactor performance represents a complex interaction between biological and physical phenomena. Physical phenomena such as shear and mixing, mass transfer and heat transfer, mostly determine the optimal microenvironment for a microorganism. Thus, reliable information on these phenomena is essential for successful scale-up or scale-down of bioprocesses. In airlift bioreactors with a dominating well-defined circulation flow, the liquid circulation is the major hydrodynamic parameter, which has considerable influence on all physical phenomena. Thus, our interest was focused to measuring techniques enabling to attain information on the residence time distribution, velocity, and the intensity of turbulence of liquid in the internal-loop ALR using a real fermentation broth.

A great number of measuring techniques has been developed in order to determine hydrodynamic parameters in bioreactors. Most of them have been applied to model media, *i.e.* water or solutions of inorganic compounds. Only few of them were used in real fermentation systems. The fundamentals of these techniques

*Presented at the 27th International Conference of the Slovak Society of Chemical Engineering, Tatranské Matliare, 22—26 May 2000.

**The author to whom the correspondence should be addressed.

***Present address*: Group of Boiengineering; Biozentrum, University of Halle, Weinbergweg 22, 06120 Halle, Germany.

Table 1. Requirements for the Use of Circulation Velocity Measurement Techniques in Fermentations

Installation	Application	Type of information
Simple	Nontoxic	Circulation velocity
Safe	Aseptic/Sterile	Residence time distribution
Fast	No interference	Velocity in main sections of ALR
Cheap	Stable for days	
Reliable	On-line	
Easy manipulation		

handicap many of them for the application in fermentations. For the selection of a suitable technique, several requirements should be formulated. The requirements can be subdivided into installation, application of the technique, and type of information obtained, as it is shown in Table 1.

One of the most important restrictions for selection of a method is that the production should not be influenced by the technique applied. The most often used measuring techniques of liquid residence time distribution are tagging techniques (pH, conductivity or heat). These methods include the labelling of liquid elements by different tracers. All of them have been successfully applied to model systems. However, during most real fermentations, the addition of any chemicals is not allowed due to the need of the strictly controlled composition of the fermentation medium. These compounds can affect not only the fermentation itself, but they can influence the transport phenomena, too. Other, more advanced measuring techniques (LDA, tomography, *etc.*) have a common disadvantage – a high price.

Another broad class of liquid velocity measuring techniques is the use of neutrally buoyant particles, the movement of which is followed by different means (radioactive counters, high-speed cameras, inductive coils, detectors of radio waves, *etc.*). Video techniques, which use coloured flowfollowers, are strongly limited by the opaqueness of fermentation broths.

A substantial problem related to the use of flowfollowers is their buoyancy. The definition of the effective buoyancy in a particle or bubble suspension is still questionable. There is a specific discrepancy in the literature; many papers claim that the buoyancy is based on the hydrostatic pressure and thus it is related to the suspension (bulk) density, *e.g.* [3—5]. This buoyancy is called the apparent buoyancy. *Schmidt* [3] corrected the measured flowfollower velocity by the settling velocity as a function of the gas hold-up and attained a good agreement with results of the pulse pH technique. Others (*e.g.* [6—8]) claim that the buoyancy force is the proper Archimedes lift force, therefore the classifying particle experiences the liquid density. However, there is circumstantial evidence that a certain criterion exists, which decides whether the particle experiences the suspension (dispersion) density or the fluid density. *Grbavcic* and *Vukovic* [6] studied the settling of the classifying particle in a fluidized bed and found that the effective buoyancy was caused by the suspension density for a particle with a diameter much larger than that of surrounding particles (more than 5 times), whereas in the case of approximately equal diameters the classifying particle experiences liquid density. *Di Felice et al.* [9] observed a similar behaviour, but they associated it with a decrease in the overall drag force, when the diameter of the classifying particle considerably exceeds that of surrounding particles. The same phenomenon but in a bubble-liquid dispersion was observed by *Middleton* [10]. It seems that there exists a *critical diameter* of the classifying particle with respect to the diameter of surrounding particles or bubbles, which determines the effective buoyancy (apparent or Archimedes buoyancy).

It is common that physical properties (pH, temperature, surface tension, viscosity) and composition of fermentation media vary during fermentation. This can considerably affect the stability and reproducibility of the measured signal; therefore, a velocity measuring technique should be independent of the fermentation characteristics, which are changing during a bioprocess.

The last demand in the application column in Table 1 should be discussed more closely:

Airlift reactors may be considered to consist of four parts, namely the riser, downcomer, the separator, and the bottom connection. However, in most studies only global values of parameters of physical phenomena (*e.g.* liquid circulation, mass transfer, and mixing intensity) are given for the reactor as a whole, despite that these parameters in the different parts differ markedly. Therefore, it seems unavoidable – at least for scale-up purposes – to study the reactor as a system consisting of interconnected subsystems [11]. To describe the operation of the bioreactor, the values of these parameters in each section need to be known.

The main goal of our study was to develop a simple and cheap method, which allows reliable measurement of the liquid circulation velocity in both vertical sections of internal-loop airlift bioreactors during fermentation processes. The flowfollowing technique using a neutrally buoyant particle with a high magnetic permeability was selected. The task was to develop a measuring system allowing to detect quickly and with a high accuracy the passing of the magnetic

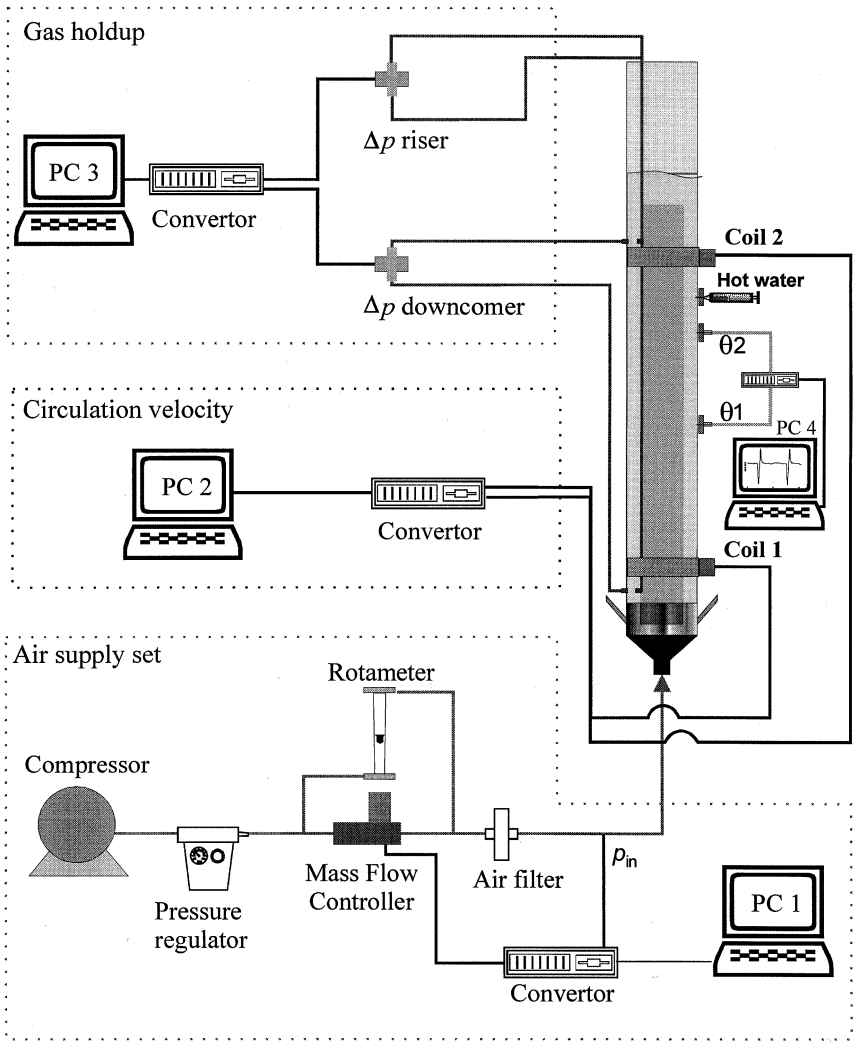

Fig. 1. Experimental set-up.

Table 2. Basic Dimensions of the Airlift Reactor

Quantity	Symbol	Size
Column diameter	D_c	108 mm
Riser tube diameter	D_R	70—74 mm
Height of the liquid level in column	H_c	1.24 m
Height of draught tube	H_R	1.15 m
Riser to downcomer cross-sectional area ratio	A_D/A_R	1.23
Aspect ratio	H_c/D_c	11.5

particle through the measurement plane. The results attained by the magnetic tracer method were analyzed and compared with the results of the commonly used pulse response technique.

EXPERIMENTAL

The measurements of the liquid circulation velocity and the gas hold-up were carried out in an internal-loop airlift reactor. A schematic diagram of the experimental set-up and details of the reactor geometry are shown in Fig. 1 and Table 2, respectively.

The total working volume of the reactor was 10.5 dm^3. Water and air as liquid and gas phase, respectively, were used in all experiments. The gas was distributed by a perforated plate with 25 holes of 0.5 mm in diameter situated at the bottom of the column. All experiments were carried out at a temperature of 18 °C and atmospheric pressure.

The air flow-rate was measured and controlled by

means of a rotameter. The gas superficial velocity, U_{GRC}, was calculated from the ratio of volumetric air flow-rate Q_G and the cross-sectional area of the riser, where Q_G was referred to the geometric centre of the column (p_C, θ_C). For each value of air flow-rate the gas hold-up, the residence time distribution of particle and liquid in individual sections of the airlift reactor were measured.

Measurement of Liquid Circulation Velocity

Liquid circulation velocity in the airlift reactor was measured by the magnetic tracer method and the commonly used pulse response method. The measuring system of the magnetic tracer method was developed according to the desired properties, which have been defined in the theoretical part. A flowfollowing technique was chosen using a neutrally buoyant particle with a high relative magnetic permeability about 8000. Two inductive coils were fixed around the column in a distance of 80.2 cm from each other to detect the transition of the magnetic tracer particle. The very important feature of our method is that the coils oscillated on *close* adjustable basic frequencies of about 130 kHz by means of oscillators. Because of the close basic frequencies, both coils are coupled together by a magnetic bond in a quasi "instable state" – where both coils try to adjust themselves to the frequency of the other. When the magnetic tracer particle travels through one of the coils, the inductivity of this increases, which causes a decrease of the frequency of the oscillations. This releases the oscillator of the second coil shifting its frequency in the opposite direction, which results in the amplification of the change of the *differential* frequency. The change of the differential frequency is measured by an A/D convertor, attached to a personal computer. For data processing a special computer program was developed.

The use of two coupled coils has further advantages – there is no need of any correction for the thermal instability of oscillators and any change of the medium composition affects both coils but not the frequency difference.

The density of the magnetic tracer particle was adjusted to the density of the liquid and a waterproof and bubble nonadherent elastomeric paint (gum-elastic) was laid on the surface of the particle. The particle size was 9 mm × 16 mm of an oval shape. The centre of gravity was placed at the side of particle.

A calibration of the measuring system was carried out and is described in detail in a previous work [12]. The accuracy of this method has been examined with a pulse response method, which is widely used for the measurement of liquid velocity in reactors. This method involves injection of a pulse of hot water into the flowing liquid. The element of hot water was detected by means of thermocouples. The distance between two thermocouples was 34.6 cm. The thermocouples were reversely connected together to one data convertor. Thus, the measured signal is a result of a difference of the signals attained from the individual thermocouples. The voltage signal from temperature sensors was scanned and processed by a data convector connected to a personal computer.

Measurement of Gas Hold-up

The gas hold-up was determined by the manometric method. Differential pressure sensors were used for the measurement of pressure differences between two places in the riser and downcomer of the ALR. The positions of measuring points were properly chosen in order to avoid the effect of a liquid acceleration at the bottom and the top of the draught tube [13]. Then, the average overall gas hold-ups, ε_{GR} and ε_{GD}, were calculated, as in *e.g.* [14].

RESULTS AND DISCUSSION

Pulse Response Method

A pulse dispersion method was used as a reference velocity measuring method. A sufficient amount of hot water was injected into the annulus and the pass of tracer element was detected by two thermocouples. The typical signal recorded by the PC is depicted in Fig. 2. Vertical positions of thermocouples are illustrated in Fig. 1.

From known time distance between adjacent peaks (t_{LD}) and the spatial distance of the thermocouples, the speed of the liquid element in the axial direction can be calculated, *i.e.* the linear liquid velocity in the downcomer V_{LD}. The time distance was determined according to the distance between the maximums of two adjancent peaks. As it has been shown by *Fields* and *Slater* [15], taking the maximum of the peaks for velocity determination is correct procedure. The same determination of the time distance was applied for the magnetic tracer method as well. The major error of the pulse method was caused by the frequency of the data processing (within 6 %).

Magnetic Tracer Method

Fig. 3 shows an example of the measured and evaluated signal, attained from both inductive coils [12]. The distance between two adjacent peaks determines the residence time of the tracer particle in the appropriate section of the ALR. A total circulation time can be calculated as a sum of residence times in all sections. Vertical positions of coils are illustrated in Fig. 1.

It can be seen that the height of peak is a function of the radial position of the particle. Thus, according to the peak height, it can be easily identified in which section of the ALR (draught tube or annulus) the par-

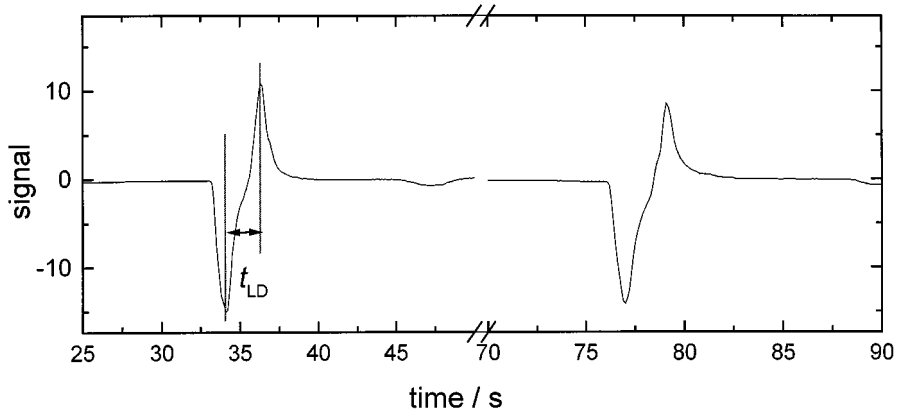

Fig. 2. Example of measured pulse signals in the internal-loop ALR determined by the pulse response technique. One double-peak represents one injection of hot water.

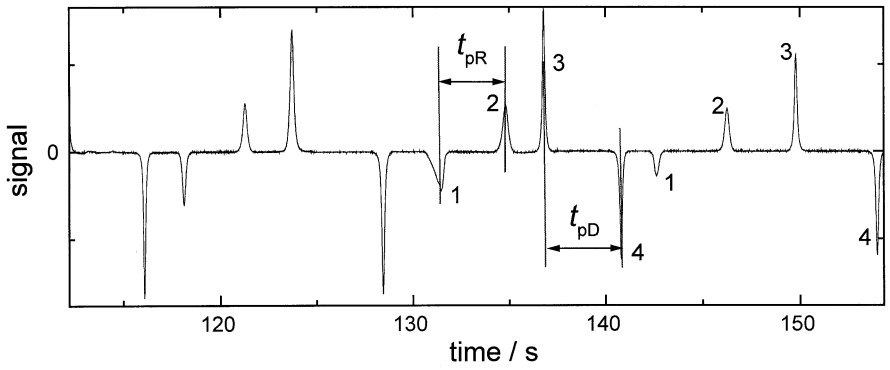

Fig. 3. Example of measured peak signals in the internal-loop ALR determined by the magnetic tracer technique. Positions of the particle: *1.* bottom of the inner tube, *2.* top of the inner tube, *3.* top of the annulus, *4.* bottom of the annulus.

ticle is actually situated. It is essential for a proper peak identification (especially in the case, when the particle passes the measuring coil more times during one circle, what may be caused by possible flow vortices).

Fig. 4 shows the effect of the superficial gas velocity on the particle residence time in the main sections of the ALR. In this figure one can see a close similarity of both curves of the residence times of particle in the vertical sections of the ALR. The residence time of the particle in the riser was about 15—24 % lower in the whole range of the air flow-rates applied. It is mainly given by the larger cross-sectional area of the downcomer (by 23 %) and the higher gas holdup in the riser. Therefore, the linear liquid velocity is larger in the riser resulting in a faster particle motion. Despite the relative sizes of vertical sections and separator, a very high residence time in the latter was observed. This was caused by the more intensive mixing in this reactor section [16], in contrary to the riser and downcomer, where a well-defined vertical flow prevails. From the known vertical distance between the measuring points L, the linear velocity of the tracer particle in the riser V_{pR} or the downcomer V_{pD} was calculated from the equation $V_{\mathrm{p}} = L/t_{\mathrm{p}}$. Basically, the magnetic particle was used as a neutrally buoyant flowfollower. However, the density of the particle was not exactly equal to the liquid density ($\rho_{\mathrm{p}} > \rho_{\mathrm{L}}$). The settling velocity of the particle in an infinite stagnant medium, U_{pt}, was measured in order to calculate the linear circulation velocity of the liquid in an appropriate section of ALR.

However, the settling of the particle is hindered by the surrounding walls as well as the present bubbles as a result of the space restriction for the particle motion. To take into account this phenomenon, the settling velocity U_{p} in the multiphase system was calculated using the modified equation of Newton [17]

$$U_{\mathrm{p}} = U_{\mathrm{pt}}(1-\varepsilon_{\mathrm{G}})k = \\ = U_{\mathrm{pt}}(1-\varepsilon_{\mathrm{G}})\frac{D^2-d^2}{D^2}\left(\frac{D^2-d^2/2}{D^2}\right)^{0.5} \quad (1)$$

Here D is the diameter of the appropriate section of the ALR and d is the particle diameter.

A hindering factor, k, is equal to 0.979 and 0.931 for the riser and the downcomer, respectively. *Di Felice* [17] examined the validity of this equation over an extensive range of d/D ratio ($0.12 < d/D < 0.92$) and found a very good agreement between this sim-

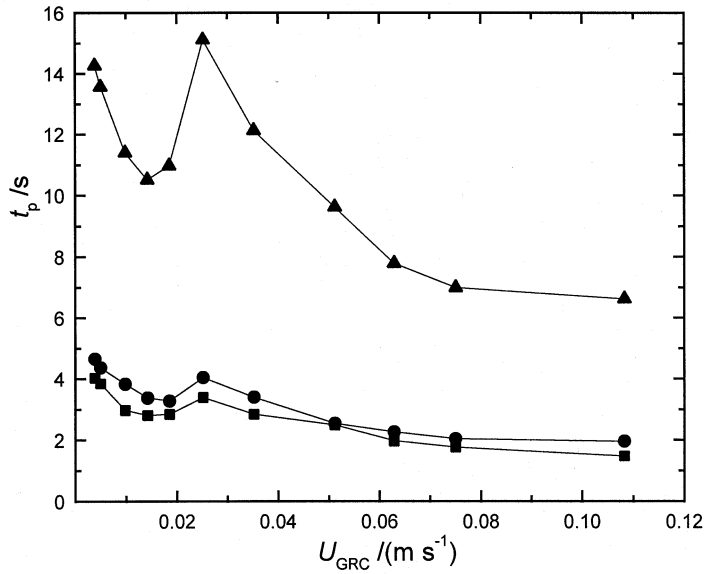

Fig. 4. The particle residence time in the main sections of the ALR as a function of the superficial gas velocity referred to the riser cross-sectional area, U_{GRC}. ■ t_{pR}, ● t_{pD}, ▲ t_{circ}.

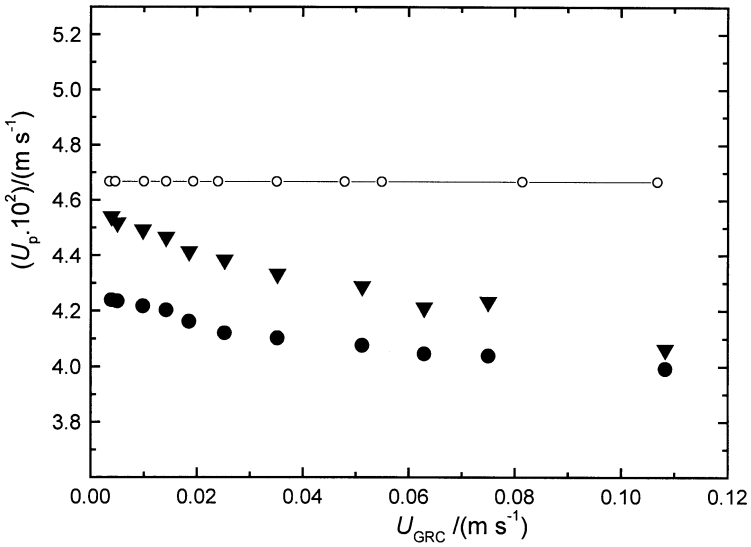

Fig. 5. Changes of the settling velocities in the riser and the downcomer with the superficial air velocity, U_{GRC}. U_{P} values were calculated from eqn (*1*). ○ U_{pt}, ● U_{pD}, ▼ U_{pR}.

ple theoretical expression and the experimental data, even for very high d/D values.

Originally, eqn (*1*) was derived for particle settling in a multiparticle suspension. Thus, we verified the validity of this expression by comparison of the experimental data of the settling of a single particle in a gas-liquid dispersion reported by *Smuk* and *Scott* [18], with the theoretical values calculated from eqn (*1*). A very good agreement (within 10 %) between experimental and calculated data was found.

Then, the linear velocity of the liquid in the appropriate section of the ALR can be calculated for the measured particle velocity V_{p} from equations $V_{\mathrm{LR}} = V_{\mathrm{pR}} + U_{\mathrm{p}}$ and $V_{\mathrm{LD}} = V_{\mathrm{pD}} - U_{\mathrm{p}}$. Here V_{LR} (V_{LD}) is the linear velocity of the liquid in the riser (downcomer).

Changes of the settling velocity (as calculated from eqn (*1*)) in the riser and the downcomer are depicted in Fig. 5. The settling velocity U_{p} falls down maximally by 20 %. Since the velocities of settling were very small in comparison with the circulation velocity, changes of the values of liquid circulation velocities by taking into account the hindering of particle motion can be neglected (up to 2.5 %). Therefore, we can use the terminal settling velocity U_{pt} to determine the linear velocity of the liquid.

Besides the indirect effect of the bubbles on the particle by space restriction for its motion, direct interactions of bubbles with the particle can occur. *Kun-*

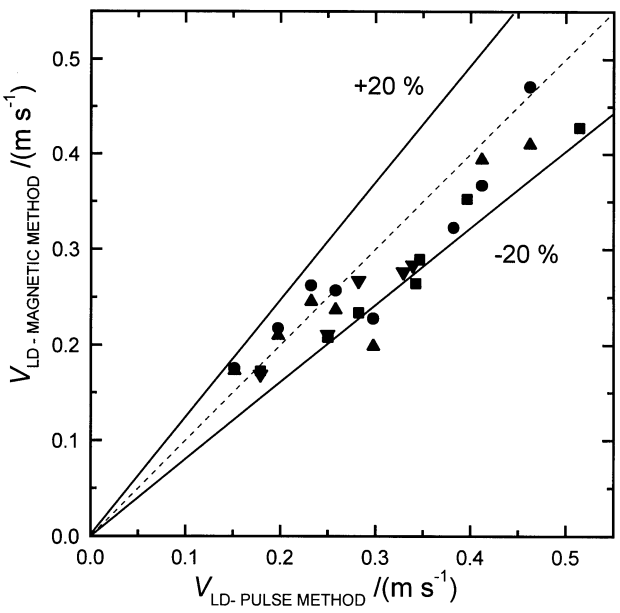

Fig. 6. The parity plot of the values of linear liquid velocity determined by pulse response and magnetic tracer methods. Symbols mark particular sets of experiments.

dakovic and *Vunjak-Novakovic* [19] pointed out that these interactions originated from a cumulative effect of the direct momentum transfer and the "lifting" of the particle by the bubbles *via* a liquid layer surrounding the bubble. The magnitude of these interactions depends strongly on the particle density. The three different settling regions for a tracer particle in two-phase and three-phase flows were identified and it was found that the bubble motion had no significant influence on the low-density particle ($\rho_p < 1100$ kg m^{-3}) and the high-density particle ($\rho_p > 1500$ kg m^{-3}) settling. The magnetic particle applied had the density equal to 1010 kg m^{-3}; therefore, no considerable interactions of bubbles with the particle are assumed.

Comparison of Measuring Techniques

Linear velocities of the liquid in the downcomer V_{LD} determined by different measuring techniques were compared. A parity plot (Fig. 6) shows a good agreement of values of V_{LD} determined by the pulse response and magnetic tracer methods and differences between measuring techniques applied do not exceed $\pm$ 20 % in most cases.

In Fig. 7 the typical dependence of V_{LD} values on the superficial air velocity U_{GRC} is shown. The standard deviations of measured V_{LD} values are plotted as error bars. The scatter of values measured by the magnetic tracer method as well as the pulse method results from the natural two-phase flow fluctuations [20]. These fluctuations affect the tracer liquid element as well as the flowfollower with the density very close to the liquid density probably in the same way.

The courses of V_{LD} values in Fig. 7 are not monotonous: at the lowest values of U_{GRC} (up to 0.02 m s^{-1}) the values of V_{LD} measured by the pulse method were little lower than those measured by the magnetic tracer technique. At $U_{GRC} = 0.02$ m s^{-1}, the largest difference between both methods appeared. An increase of air flow-rate had opposite effect on the measured liquid circulation velocity: the value of V_{LD} measured by the pulse method increased, while in the case of the magnetic tracer method it decreased. At

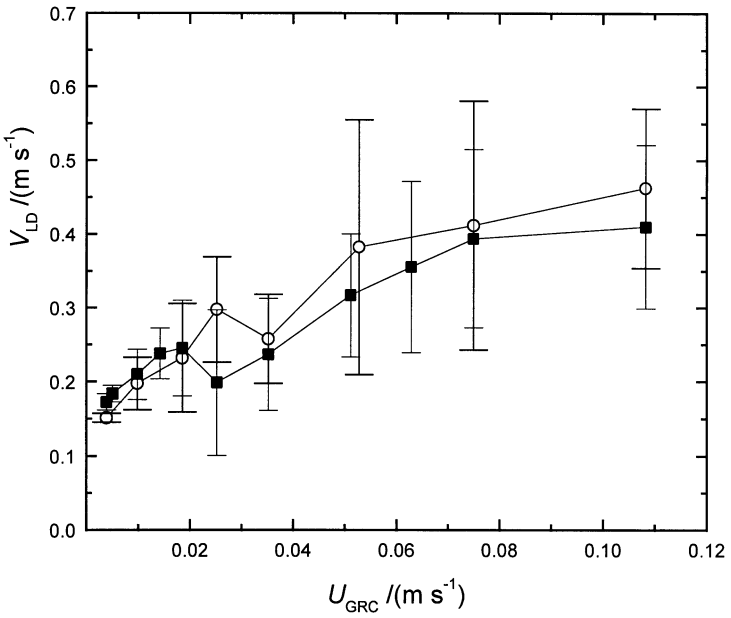

Fig. 7. The linear liquid velocity as a function of the superficial air velocity U_{GRC} determined by different measuring techniques. Error bars indicate the standard deviations of measured values. ○ V_{LD} (pulse method), ■ V_{LD} (magnetic method).

Table 3. Survey of Papers, in which the Change of V_{LD} Values Corresponding to the Onset of the Bubble Recirculation Was Observed

Ref.	ALR type	Technique used for the liquid velocity measurement
van Benthum et al. [21]	IALR	Electromagnetic velocity probe
Klein et al. [22]	IALR	Flowfollower – magnetic method
Jones [23]	IALR	Flowfollower – visually
Kennard and *Janekeh* [24]	IALR	Flowfollower – visually
Merchuk et al. [25]	IALR	Pulse tracer method – pH
Bakker et al. [26]	IALR	Pulse tracer method – pH
Snape et al. [27]	EALR	Pulse tracer method – conductivity
Weiland [16]	IALR	Pulse tracer method – conductivity
Barker and *Worgan* [28]	IALR	Pulse tracer method – hot water

IALR – internal-loop airlift reactor, EALR – external-loop airlift reactor.

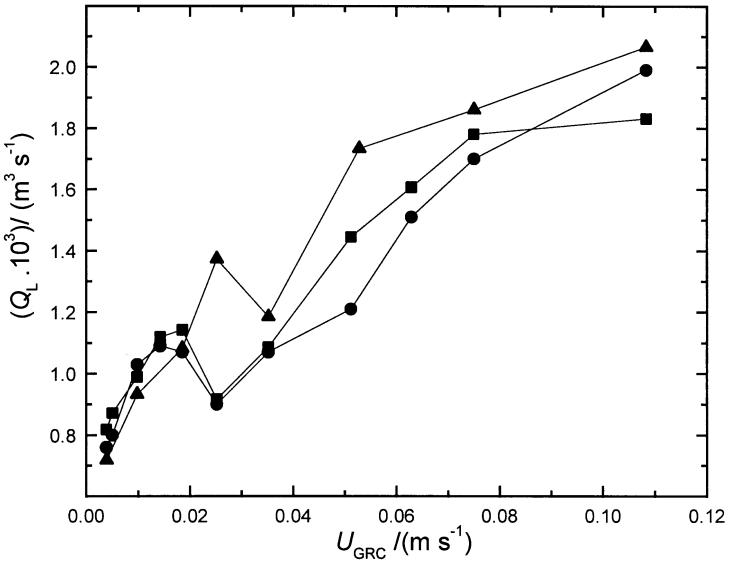

Fig. 8. Liquid flow-rates in the riser (Q_{LR}) and downcomer (Q_{LD}) of ALR determined by both measuring techniques. ■ Q_{LD} (magnetic tracer method), ● Q_{LR} (magnetic tracer method), ▲ Q_{LD} (pulse tracer method).

the highest values of U_{GRC} (higher than 0.035 m s^{-1}), the values of V_{LD} measured by the pulse method were somewhat higher. Very similar courses of V_{LD} values have been observed in all experiments. This sudden change in the course of V_{LD} corresponds exactly to the onset of bubble recirculation into the riser [21]. A decrease of the value of V_{LD} at this point of the regime transition can be found in other papers as well; even if mostly not commented. A survey of related papers is listed in Table 3.

The same trend of V_{LD} curves – a plateau and then a slight or stronger decrease before the onset of the bubble recirculation, was measured using different measuring techniques. Thus, it seems that this abrupt change on the V_{LD} curve corresponding to the circulation regime transition is not a particular feature of flowfollowing techniques, but it is a characteristic phenomenon of a certain design of internal- as well as external-loop airlift reactors.

As a next criterion, which can confirm the consistency of the measured values of liquid circulation velocities using the magnetic tracer method, the equality of the liquid flow-rates in the riser and the downcomer was chosen. Since the velocities in both the sections of the ALR were measured, the liquid flow-rate could be calculated from a simple equation $Q_{LR(D)} = V_{LR(D)} \cdot A_{R(D)}$. Fig. 8 shows the values of liquid flow-rates in the riser (Q_{LR}) and the downcomer (Q_{LD}) determined by the magnetic tracer method and Q_{LD} values specified by the pulse method. It can be seen that the liquid flow-rates in the main sections of ALR agree well in the whole range of the air flow-rates. Q_{LD} values measured by the pulse method were somewhat higher, as in Fig. 7.

The differences between the values obtained by the two methods may be explained as follows: The linear velocity V_{LD} was measured by the pulse method in the upper part of the column, whereas the measuring coils used by the magnetic method were situated at the bottom and the top of the downcomer. At low air

flow-rates, when the gas hold-up is very small, the differences between V_{LD} values measured by both techniques are very small. However, when the bubbles are entrained into the downcomer and an axial distribution of gas hold-up appears, the linear liquid velocity in the upper part is higher than the velocity averaged along the whole downcomer. The existence of axial distribution of gas hold-up is not caused by a hydrostatic pressure change only, but also by a higher concentration of bubbles in the upper part of the downcomer.

Effect of G-L Dispersion on Particle Motion

In order to test, which effective buoyancy force affects the motion of our magnetic tracer particle, the settling velocity of the magnetic particle U_p for both considered cases of the bouyancy definition was calculated using the well-known expressions [29]. The density of the gas-liquid dispersion in the appropriate section of the ALR (ρ_{disp}) was calculated from the measured value of the gas hold-up. Applying this density, the values of the settling velocities U_{p-disp} were calculated. Then, the linear liquid velocity in the downcomer was determined from the well-known equations. The same procedure was applied, when the liquid density was considered.

In addition, the equation of continuity was applied to the main sections of the airlift reactor to verify the validity of formulation of the effective buoyancy. Since all variables in the equation were measured, the "theoretical" values of the liquid circulation velocity in the downcomer V_{LD-CAL} can be calculated and compared with measured values of V_{LD}

$$V_{LD-CAL} = V_{LR}\frac{A_R(1-\varepsilon_{GR})}{A_D(1-\varepsilon_{GD})} \qquad (2)$$

Here A_R and A_D are the cross-sectional area of the riser and the downcomer, respectively.

The measured and calculated values of V_{LD} for both possible cases of the formulation of the effective buoyancy are shown in Fig. 9. The graph clearly demonstrates that in the case of the validity of the apparent buoyancy, the differences between calculated and measured values of V_{LD} are much greater than in the case of application of Archimedes buoyancy. Therefore, it can be concluded that the magnetic particle experiences the liquid density and the Archimedes buoyancy is the correct effective buoyancy affecting the motion of the particle in the G-L dispersion. It is in accordance with findings of *Middleton* [10] and *Grbavcic* and *Vukovic* [6]. They claim that the flowfollower experiences the liquid density, when the particle size is about equal to the average bubble size. In this study, the particle had a size of 9 mm × 16 mm, whereas the air in tap water formed bubbles of equilibrium size of 6 mm. At higher values of air flowrates besides these bubbles also coalescing bubbles of greater diameter (up to about 40 mm) occurred. It can be concluded that the magnetic tracer technique gives correct results of the linear circulation velocities of liquid in the range of our investigated conditions, when the liquid density is applied to determine the effective buoyancy.

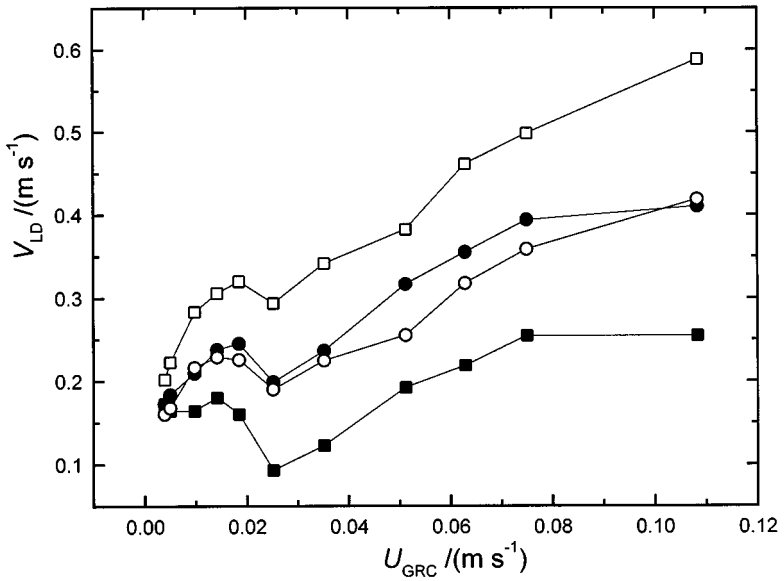

Fig. 9. Experimental and calculated values of V_{LD} for both possible cases of formulation of the effective buoyancy (apparent and Archimedes buoyancy) as a function of U_{GRC}. ■ Experimental value corrected for the dispersion (G-L) density $V_{LD-disp}$, □ value calculated from eqn (*2*) with the correction for the dispersion (G-L) density, ● experimental value corrected for the liquid (L) density, ○ value calculated from eqn (*2*) with the correction for the liquid (L) density.

CONCLUSION

The magnetic tracer method was developed according to the defined requirements for the measurement of the liquid circulation velocity in the individual sections of the internal-loop airlift bioreactors during the fermentation process. All selected demands on the measuring technique were fulfilled. The magnetic tracer method was tested for the model media with the aim of a detailed analysis of measured experimental data. Using the method, a signal with a very low noise was attained, which gave reproducible information on the residence time of the magnetic particle in the appropriate section of the ALR. Effects of reactor walls and surrounding bubbles were taken into account in order to calculate the settling velocity of the magnetic particle U_{p}. A comparison of the calculated settling velocity U_{p} and the terminal settling velocity U_{pt} showed a maximal difference of 20 %. However, since the settling velocities of almost neutrally buoyant magnetic particle were very small in comparison with the attained liquid velocities, changes of the values of liquid circulation velocities by taking into account the hindering of particle motion could be neglected (up to 2.5 %). It means that if the density of the tracer particle is adjusted very close to the fluid density, it is not necessary to take into account the hindering effects on the particle and the terminal settling velocity can be used to calculate the liquid velocity.

The magnetic tracer technique was compared with the common pulse response method using hot water. Results showed that the magnetic method is suitable for the measurement of linear circulation velocities of liquid in the ALR. Differences of V_{LD} values between both measuring methods were within ± 20 %. Following the equation of continuity, the liquid flow-rates in the riser and downcomer of ALR should be equal. A good agreement was attained for all experimental data measured by the magnetic tracer technique.

Moreover, the effect of the gas-liquid dispersion on the particle settling was investigated. Our results demonstrate that the effective buoyancy is based on the liquid density, so the Archimedes buoyancy force is a proper expression for the formulation of the effective buoyancy. It is in accordance with numerous papers, however, many other papers showed contrary conclusions, *i.e.* the effective buoyancy is based on the dispersion (suspension) density. It seems that probably a *critical diameter* of the classifying particle with respect to the diameter of surrounding particles or bubbles exists, which determines the formulation of the effective buoyancy [6, 9, 10]. If the classifying particle is much greater (several times) than the surrounding bubbles, the particle experiences the G-L dispersion density; otherwise it experiences the liquid density. In our case the size of the magnetic particle was comparable with the average bubble size. Thus, our results confirmed this implication. However, further experiments with different sizes of the magnetic tracer particle have to be carried out to verify reliably the correct formulation of the effective buoyancy. An applicability of the usage of the magnetic tracer method will be tested for various fermentation processes.

Acknowledgements. This work was supported by the project Copernicus IC15-CT98-0904 and Grant 1/7352/20. We thank J. Annus and Š. Pollák for a construction of the equipment for measuring liquid velocity and for providing the data acquisition and PC software.

SYMBOLS

A	area or cross-sectional area	m^2
d	diameter of particle	m
D	diameter of reactor section	m
H	height	m
k	hindering factor	
L	vertical distance	m
p	pressure	Pa
Q	volumetric flow-rate	$m^3\ s^{-1}$
t	time	s
θ	temperature	℃
U	superficial velocity	$m\ s^{-1}$
U_{p}	settling velocity of particle	$m\ s^{-1}$
U_{pt}	terminal settling velocity of particle	$m\ s^{-1}$
V	linear velocity	$m\ s^{-1}$

Greek Letters

ε	hold-up	
ρ	density	$kg\ m^{-3}$

Subscripts

B	bottom
b	bubble
c	column
C	characteristic value, referred to the geometric centre of the column
disp	G-L dispersion
D	downcomer
G	gas phase
L	liquid phase
p	particle
R	riser

REFERENCES

1. García-Calvo, E. and Letón, P., *Chem. Eng. Sci. 46*, 2947 (1991).
2. Verlaan, P., Tramper, J., and van't Riet, K., *Chem. Eng. J. 33*, B43 (1986).
3. Schmidt, K. G., *Verfahrenstechnik 17* (10/11), 593 (1983).
4. van der Wielen, L. A. M., van Dam, M. H. H., and Luyben, K. C. A., *Chem. Eng. Sci. 51*, 995 (1996).
5. Gibilaro, L. G., Di Felice, R., Waldram, S. P., and Foscolo, P. U., *Chem. Eng. Sci. 42*, 194 (1987).

6. Grbavcic, Z. B. and Vukovic, D. V., *Chem. Eng. Sci. 47*, 2120 (1992).
7. Clift, R., Seville, J. P. K., Moore, S. C., and Chavarie, C., *Chem. Eng. Sci. 42*, 191 (1987).
8. Fan, L.-S., Han, L. S., and Brodkey, R. S., *Chem. Eng. Sci. 42*, 1269 (1987).
9. Di Felice, R., Foscolo, P. U., and Gibilaro, L. G., *Chem. Eng. Process. 25*, 27 (1989).
10. Middleton, J. C., in *Proceedings of 3rd European Conference on Mixing*, Vol. *A2*, 15 (1979).
11. Merchuk, J. C. and Berzin, I., *Chem. Eng. Sci. 50*, 2225 (1995).
12. Godó, Š., Annus, J., Pollák, Š., Dolgoš, O., and Klein, J., in *Proceedings of 26th Conference of SSChE*, CD ROM with full texts, 7 pp. Jasná, Slovakia, 1999.
13. Merchuk, J. C., Ladwa, N., Cameron, A., Bulmer, M., and Pickett, A., *AIChE J. 40*, 1105 (1994).
14. Chisti, Y., *Airlift Bioreactors*, p. 345. Elsevier Science Publishers, London, 1989.
15. Fields, P. R. and Slater, N. K. H., *Chem. Eng. Sci. 38*, 647 (1983).
16. Weiland, P., *Ger. Chem. Eng. 1984,* 374.
17. Di Felice, R., *Chem. Eng. Sci. 50*, 3005 (1995).
18. Smuk, D. and Scott, D. S., *Can. J. Chem. Eng. 69*, 1382 (1991).
19. Kundakovic, L. and Vunjak-Novakovic, G., *Chem. Eng. Sci. 50*, 3285 (1995).
20. van der Lans, R. J. G. M., *Ph.D. Thesis*. Delft University of Technology, Delft, The Netherlands, 1985.
21. van Benthum, W. A. J., van der Lans, R. G. J. M., van Loosdrecht, M. C. M., and Heijnen, J. J., *Chem. Eng. Sci. 54*, 3995 (1999).
22. Klein, J., Godó, Š., Dolgoš, O., and Markoš, J., in *Proceedings of 46th Congress of CHISA*, CD ROM with full texts, 15 pp. Srní, Czech Republic, 1999.
23. Jones, A. G., *Chem. Eng. Sci. 40*, 449 (1985).
24. Kennard, M. and Janekeh, M., *Biotechnol. Bioeng. 38*, 1261 (1991).
25. Merchuk, J. C., Contreras, A., Garcia, F., and Molina, E., *Chem. Eng. Sci. 53*, 709 (1998).
26. Bakker, W. A. M., van Can, H. J. L., Tramper, J., and Gooijer, C. D. D., *Biotechnol. Bioeng. 42*, 994 (1993).
27. Snape, J. B., Zahradník, J., Fialová, M., and Thomas, N. H., *Chem. Eng. Sci. 50*, 3175 (1995).
28. Barker, T. W. and Worgan, J. T., *Eur. J. Appl. Microbiol. Biotechnol. 13*, 77 (1981).
29. Perry, R. H., *Perry's Chemical Engineers' Handbook*. McGraw-Hill, New York, 1985.